Surface morphology and formation of GaAs nanocrystals by laser-induced etching: SEM, PL and Raman studies

H.S. Mavi[a,*], A.K. Shukla[a], B.S. Chauhan[b], S.S. Islam[b]

[a] *Department of Physics, Indian Institute of Technology, Hauz Khas, New Delhi-110016, India*
[b] *Department of Applied Sciences and Humanities, Jamia Millia Islamia, New Delhi-110025, India*

Received 21 May 2003; accepted 20 October 2003

Abstract

GaAs nanostructures were prepared by a laser-induced etching process using aNd: YAG (λ = 1.06 fim) laser. Scanning electron microscope (SEM) was used to monitor changes in surface morphology produced on etching. The etched samples were subjected to photoluminescence (PL) and Raman spectroscopic investigations using an argon-ion laser of excitation energies of 2.54 and 2.71 eV. PL spectra from etched GaAs shows two broad luminescence bands along with a red shift in comparison to a sharp band in the unetched GaAs. Raman measurements exhibit enhancement of first-order LO mode peak intensity in the etched sample along with line-shape asymmetry and shifting of mode towards lower frequency with increasing laser excitation energy. Both Raman and photoluminescence results were explained using quantum confinement models involving Gaussian size distribution of nanocrystallites constituting of GaAs nanostructures. There is reasonable agreement between the results obtained from photoluminescence and Raman spectroscopic investigations of the etched GaAs samples.

Keywords: **Nanostructures; Raman scattering; Photoluminescence; GaAs**

1. Introduction

The increasing interest in low-dimensional semiconductor structures is mainly motivated by the search of materials with tunable optical properties of evident technological relevance. Semiconductors nanocrystallites, in general, porous silicon [1], and GaAs [2] nanocrystalline materials have been the subject of intense studies over the last decade primarily due to their interesting size dependent electronic and optical properties. Blue-shift of the optical absorption spectrum, size dependent luminescence, enhanced oscillator strength, non-linear optical effects are some examples of the interesting properties exhibited by these nanostructures. Laser-induced etching of silicon in the liquid etchants has been used to create silicon nanocrystals [3-6]. In GaAs, most of the work has been performed with the aim to remove GaAs by layer-by-layer etching [7-11] and no vibrational studied have been reported on the etched samples to best of our knowledge. Direct band gap semiconductors, such as GaAs [12-14], would be of interest in nanotechnology, if one can enhance the band gap in the nanocrystals by laser-induced etching or by any other process.

Several approaches have been developed for the synthesis of GaAs nanostructures including laser ablation [15], sequential ion-implantation [16-18], magnetron co-sputtering [19], and electrochemical etching [20,21]. Perriere et al. [15] have fabricated the GaAs nanocrystals by the laser ablation. Photoluminescence (PL) spectra shows PL peaks shift about 870 meV higher energies compared to bulk GaAs (1.515 eV at 10K). They have shown that this increase in the energy is due to confinement effect of electron and estimated sizes around 6nm. Sabataityte et al. [21] have synthesized porous GaAs by anodic etching in HF solution and their TEM studies provides the nanometer size GaAs nanocrystals and pore. They observed a strong PL band at 778 nm and was explained by quantum size effect. Kanemitsu et al. [16-18] have studied the mechanism of visible broad PL in the red spectral region of GaAs nanocrystals in SiO2 matrices formed by sequential ion-implantation. They proposed that the red PL is due to free-exciton and bound-exciton emission in the GaAs nanocrystals.

In this work, we have fabricated GaAs nanostructure by laser-induced etching using Nd:YAG (λ = 1.06 (xm) laser, which is probably a simplest technique to produce nanocrystallites and sizes can be controlled by changing laser parameters.

Raman spectroscopy [13] provides a rapid, non-destructive, and simple diagnostic method for determining the nanocrystal dimensions and is a potential process-control tool during laser generation of nanocrystals. Basically, confinement of the electrons and phonons in reduced dimensional systems lead to major modifications in their electronic and vibrational properties. The vibrational modes, observed in the Raman spectra, are sensitive to the sizes. Different sizes of nanocrystallites will affect the shift, broadening, and lineshape of the Raman signal in different ways. Therefore, changes in the line broadening and peak position of the optical phonon mode observed in the Raman spectra can be used as an indirect measurement for the shape and dimensionality of nanocrystallites.

Photoluminescence spectroscopy is a sensitive probe of the electronic states and can be suitably used to characterize nanostructures. The broad PL band from etched silicon or nanocrystalline silicon is explained under the assumption that etched silicon contains a distribution of nanocrystallites with different sizes [22,23]. The position and shape of the PL band is determined by the size distribution of crystallites. The relationship between the PL peak energy and the mean radius of crystallites has been studied by many authors [4,22-24] for nanocrystalline silicon and similar approach can be used for etched GaAs. The measured energy corresponding to the peak position of the PL band increases as the nanocrystallite average size decreases.

In this paper, we propose a method for the formation of a layer of GaAs nanocrystals on GaAs substrate by the laser-induced etching. The information regarding the surface morphology can be obtained by using scanning electron microscopy (SEM). Photoluminescence and Raman spectroscopic studies are also reported to examine the formation of nanocrystallites in the GaAs after laser etching. The size and size distributions estimated by the analysis of the PL and Raman data using the existing quantum confinement models agree reasonably well.

2. Experimental procedure

2.1. Sample preparation

Fig. 1 shows a schematic diagram of the experimental set-up for the laser induced etching. A commercially available Cr-O doped GaAs (10 0) wafer with resistivity of 10^7 Q. cm was immersed in hydrofluoric acid with 40% concentration placed in a plastic container and was supported on two Teflon plates. The Cr content in the sample was roughly to 1 wt. ppm. Laser etching was done by using a Nd:YAG

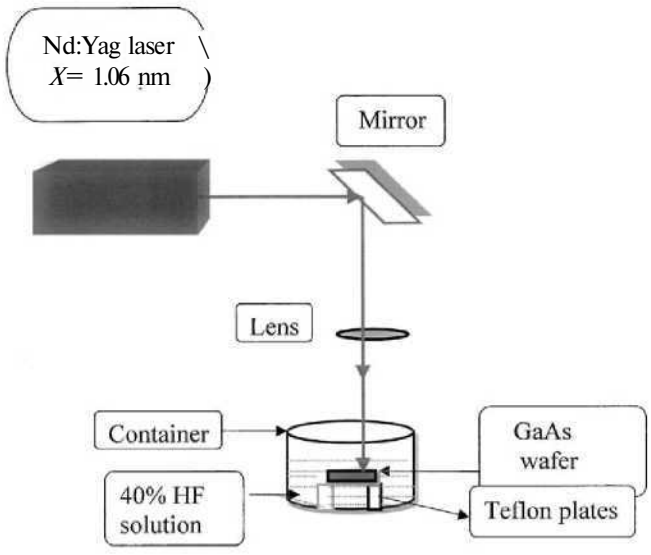

Fig. 1. Scheme of experimental laser etching set-up.

($_\lambda$ = 1.06 (xm) (Quantronix, model 331) laser in CW mode. The beam was focused to a circular spot of 1.5 mm diameter. The sample was irradiated with a laser power density of 20 W/cm^2 for duration of 60 min to etch above mention GaAs wafer. After etching, the sample was rinsed with ethanol and dried in air with filtered N2. The surface morphology of the etched GaAs was studied by SEM (Cambridge Instrument, Stereoscan 360).

2.2. Experimental set-up

The PL and Raman spectra were recorded by employing a spectroscopic system which consisted of a RAMANOR double monochromator (HG 2S), a HAMAMATSU R943-2 photomultiplier tube, an amplifier-discriminator assembly, a photon counter, a computer and an argon-ion laser (COHERENT, INNOVA 90-5) light source. The double monochromator included holographic gratings blazed for 5000 Å designed to produce a net dispersion of 2.5 Å/mm. The monochromator was calibrated using a low pressure Cd-Hg lamp as well as by recording the plasma lines from the discharge in the argon-ion plasma tube. The instrumental line width obtained by using 100 (xm slits was estimated to be better than 0.5 cm («a0.06 meV). The resolution of the spectrometer was also checked by recording the fine structure of the CCl4 line at nearly 459 cm and the resolution was estimated to be «»0.5 cm^{-1} when a slit width of 100 (xm was used. The samples were excited by the 457.9 (2.71 eV) and 488 nm (2.54 eV) lines of a CW argon-ion laser. Raman and PL spectra were recorded with 100 (xm slit width for the spectrometer. In order to avoid thermal heating, the power of laser light on the sample surface was 100 mW on a spot with a diameter of 100 (xm.

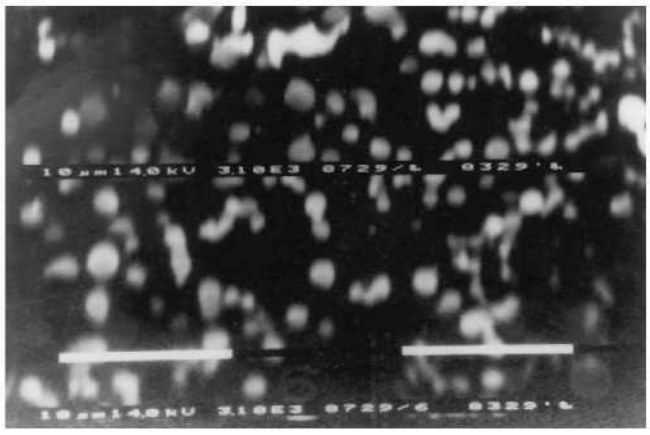

Fig. 2. SEM image of GaAs surface etched by laser power density 20W/cm^2 from Nd:Yag laser (λ = 1.06 [xm) for irradiation time 60min.

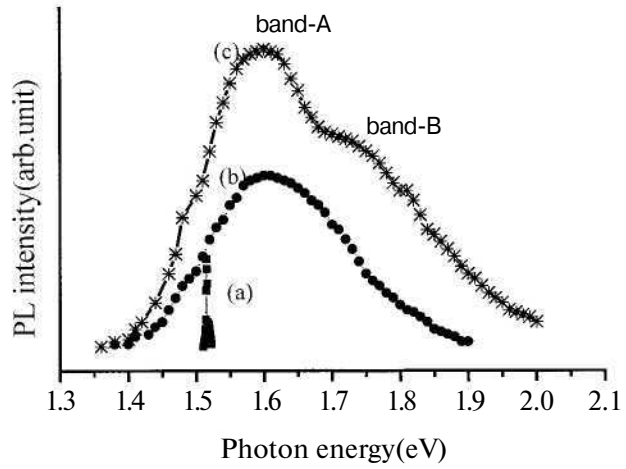

Fig. 3. (a) PL spectra of unetched GaAs sample at 20 K, where (b) and (c) are the PL spectra of GaAs after etching recorded with laser excitation energies 2.71, and 2.54eV at 20 K, respectively.

3. Experimental results and discussion

3.1. Surface morphology

Fig. 2 shows the SEM image of the etched GaAs wafer prepared by laser-induced etching using a Nd:YAG laser (λ = 1.06 (xm) in the HF etching solution. At the top surface, microcrystallites of micrometer size with pits were observed. The thickness of the etched layer is about 3 (xm measured by optical microscope and is quite uniform. The SEM micrograph shows relatively microstructures of size ~10(im. The developed pits and their structures shown in Fig. 2 are practically identical to Fig. 1 (SEM image of GaAs nanocrystals) of [21], though, they have prepared sample by anodic etching. In etching process, arsenic atoms are etched away faster than the gallium atoms, which will change the surface stoichiometry. The pit formation is accompanied by the formation of GaAs nanostructures. Therefore, optical characterization techniques such as the photoluminescence and Raman scattering could be useful to study the changes in the etched GaAs samples.

3.2. Photoluminescence

Fig. 3 shows the PL spectra of GaAs sample at temperature 20 K before and after etching. The PL spectrum of the unetched GaAs sample consist of a peak at 1.515 eV with full width at half maximum (FWHM) of 3 meV is shown in Fig. 3(a). It is attributed to recombination process of the free carriers in GaAs. We do not see any other emission. Fig. 3(b) and (c) shows the PL spectra of the etched GaAs sample recorded with laser excitation energies of 2.71 and 2.54 eV, respectively at 20 K. The spectra recorded with laser excitation energy 2.54 eV show broad luminescence band of FWHM 300 meV with a tail towards higher energy side shown in Fig. 3(b). The maxima of the PL peak is at 1.6 eV and is blue-shifted roughly 100 meV Besides, the peak energy of the PL band (1.6 eV) is above the exciton energy of bulk GaAs unetched sample (1.515 eV). In molecular terminology, this corresponds to the widening of the energy gap between the highest occupied molecular orbital and the lowest unoccupied molecular orbital as the size decreases. Therefore, one may believe that the efficient red PL (1.6 eV) is related to the quantum confinement state of GaAs nanocrystals. However, this broad PL spectra can be divided into two bands: one at 1.6 eV (band-A) in the near IR and other at 1.8 eV (band-B) in the visible red region. These observations concerning the two PL bands and their positions are quite similar to GaAs nanocrystals formed by sequential ion-implantation of Ga^+ and As^+ in SiO2 film on silicon substrate and followed by thermal annealing [18]. Kanemitsu et al. [18] have shown that the band-B is due to the delocalized exciton (free-exciton) emission in quantum confined GaAs nanostructures. The low energy band-A is attributed to localized exciton (bound-exciton) emission in shallow trap and impurity states in the GaAs nanocrystals. Our results presented here are in full agreement with [18].

It has been shown [17,18,21] that the GaAs nanocrystals emit visible luminescence in the samples. Moreover, the luminescence peak energy is above the band gap of bulk GaAs. Visible luminescence from nanocrystals is often attributed to quantum confinement effects. It has been proposed that electronic confinement within nanometer size crystallites leads to a blue-shift of the band gap to the visible region. However, the confinement effect cannot alone explain the broad PL spectrum which typically exhibits a FWHM of 150 to 300 meV. There have been suggestions, that a distribution of crystallite sizes may be responsible for the broad band [22,23]. The size of nanocrystallites can be determined by a model proposed by Suemoto et al. [22], assuming that each particle constituting nanocrystallites gives sharp luminescence. For a size distribution function *D(R),* the PL intensity

$S(E)$ can be written as:

$$S(E) = ca(E_{exe}\text{-}E)D(R)\frac{1}{nE\text{-}E_g}\frac{R_E}{} \quad (1)$$

where RE is the crystallite radius defined by $RE = \{\gamma/(E - Eg)^{1/n}\}$, and $n = 2$. The E_g0 is the gap energy of bulk GaAs. The $(E - £g)$ is inversely proportional to the square of radius of the crystallites. The coupling constant γ is in electronvolt $(Å)^2$, while $Eg0 = 1.42$ eV at room temperature. The c is a constant, which includes an intensity of light source at excitation energy E_{exc}. The $\alpha(E_{exc} - E)$ is the absorption coefficient. The function $\alpha(E)$ can be reduced to simple form such as $\alpha(E) = a1 + a2E^2$, where $a1$ and a2 are constants. The function $D(R)$ is taken here as a Gaussian distribution function $[\exp - ((R - R0)/\sigma)^2]$, to analyze our data and σ is the standard deviation. For excitation energy 2.54 eV, the PL spectra shows two clear bands around 1.6 and 1.8 eV in Fig. 3(c). Each band has its different origin; one is due to free exciton and other is due to bound-exciton. Therefore, we will have two different set of distribution of nanocrystallite in the etched GaAs sample and cannot be fitted with single Gaussian distribution. If we assume single Gaussian distribution, it leads to a large deviation to fitted results in Eq. (1). Therefore, we assume, two Gaussian distributions and each one is fitted with Eq. (1). The calculated excitonic energy spectrum for both Gaussian distribution of our sample is shown by dotted line in Fig. 4(a). Finally, if we take convolution of both excitonic spectrum, we can fit our experimental data of Fig. 4(a) and various parameter are given in Table 1. The theoretically calculated shapes of PL bands are drawn as continuous curves in Fig. 4(a) and (b). The experimental data (solid stars) has a reasonably good fitting with the theoretical results. Therefore, we conclude that Table 1 gives the nanocrystallite size distributions obtained by using Eq. (1). Similarly, for laser excitation energy 2.71 eV, the PL spectra of the same sample is shown in Fig. 4(b). The sample shows a broad luminescence band with peak energy at 1.6 eV in the red spectral region. In GaAs semiconductors, the PL intensity due to excitons bound to impurities is sensitive to the hydrogen concentration in the sample [18]. Since, our sample also has been etched in 40% HF concentration, therefore, we expect the top layer of GaAs nanocrystals may be hydrogenated along with impurities and defects.

Table 1
PL fitting parameters of band A and band B for GaAs etched samples for two excitation photon energies

Band	Excitation energy (eV)	Theoretical		Experimental
		$L_0 = 2R0$ (Å)	σ (Å)	PL peak position (eV)
A	2.54	46	50	1.6
B	2.54	35	20	1.8
A	2.71	54	50	1.55
B	2.71	40	50	1.65

Where σ is the standard deviation of the Gaussian distribution $D(R)$ used in Eq. (1).

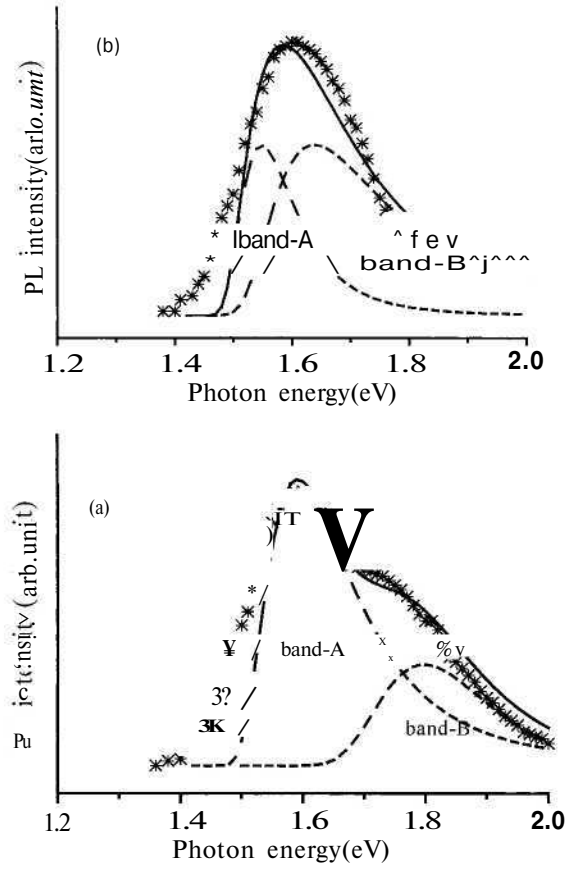

Fig. 4. PL spectra of etched GaAs sample, where (a) and (b) are the PL spectra recorded with excitation photon energies 2.54 and 2.71 eV, respectively. Experimental data are plotted as discrete points (solid stars) and calculated PL spectra using Eq. (1) are given by solid curves.

On changing excitation energy from 2.54 to 2.71 eV, the penetration depth [25] of laser light decreases from 0.05 to 0.02 (xm and top layer of etched GaAs is excited; consequently, the PL for free-excitons and bound-excitons become closer and comparable to each other as shown in Fig. 4(b). Fitted results of the PL spectrum are given in the Table 1. It shows same standard deviation $(\sigma = 50$ A) values for both types of exciton. In contrast, for excitation energy 2.54 eV, it shows two different values. Basically, it is inhomogeneous distribution of bound-exciton and free-exciton of nanocrystallites in laser etched GaAs sample, which shows different shape of the PL spectra depending upon penetration depth of laser light. One can say that the changing excitation energy excites the nanocrystals of specified range of diameter.

4. Raman scattering

The Raman spectra at room temperature of GaAs before and after etching are shown in Fig. 5. Fig. 5 (a) shows the first-order Raman spectrum [13] of the unetched sample at room temperature. It consists of a peak at 291cm"[1] with

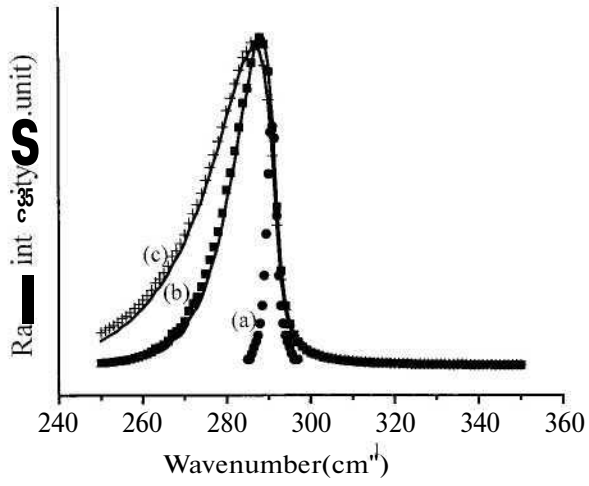

Fig. 5. Raman spectra of unetched crystalline GaAs sample at room temperature is shown in (a), where (b) and (c) are comparison of experimental (solid stars recorded with excitation energy 2.71 eV and solid squares recorded with excitation energy 2.54 eV) and theoretically calculated Raman spectra for etched samples using Eq. (2). Calculated Raman spectra are indicated by smooth line curves and experimental data are plotted as discrete points.

a FWHM (3.5 cm^{-1}) corresponds to the LO phonons associated with the Brillouin zone-center. In zinc-blend type crystals the optical phonons near $_{\Gamma}$-point spilt into TO and LO phonons by the microscopic electric field. The only Raman band allowed in back scattering geometry by a (10 0) surface of GaAs is the LO phonon and TO phonon being forbidden by symmetry selection rules. The main parameters characterizing the Raman bands are the peak position and the line-shape. Therefore, a careful analysis of these spectral parameters together with the selection rules is required to extract information on the pre and post etching results. Fig. 5(b) shows the Raman spectrum for the etched GaAs samples prepared by Nd: YAG laser. The spectra were recorded by employing laser photon energy of 2.54 eV from an argon-ion laser. There is a shift in the Raman LO mode to a lower frequency 288 cm and enhancement of peak intensity after etching. Furthermore, the Raman line is wide and asymmetric in comparison to that of crystalline unetched GaAs for which the line is narrow and symmetric, centered at 291 cm"[1]. Furthermore, the line-shape asymmetry increases as the incident photon energy increases from 2.54 to 2.71 eV in Fig. 5(c). The changes observed in the Raman line-shape as a function of laser excitation energy may be attributed to the spatially dependent size distribution of nanocrystallites in our sample. The line-shape asymmetry ratio $\Gamma a/\Gamma_b$ (Γ_a and Γ_b being the half width on the low- and high-energy sides from the center of the peak position, respectively) increases from a value 2.60 for 2.54eV to 3.1 for 2.71 eV of laser excitation energy. The smaller asymmetry ratio in the Raman line obtained with 2.54 eV implies larger nanostructure sizes deeper inside the sample compared to those in upper layers of the nanostructure surface. This is due to the fact that the penetration depth is larger at 2.54 eV compared to that of at 2.71 eV of photon energy. The enhancement of peak intensity in etched sample is attributed to the increase of Raman efficiency for smaller particles and large quantum confinement factor.

The size of nanocrystals can be determined by employing the phonon confinement model [26,27]. This model is based upon the fact that optical phonons at the center of the Brillouin zone ($\vec{q} = 0$) contribute to the first-order Raman mode at 291cm"[1] of the crystalline GaAs. For nanocrystals, the momentum conservation criterion is relaxed and no longer valid because optical phonons are localized within the nanostructures. This also allows optical phonons with ($\vec{q} \neq 0$) to contribute to the Raman mode. Therefore, the first-order Raman intensity / (&, *L)* is given by

$$I'(\omega, L) \alpha \int_{L_1}^{L_2} N(L)dL \int_{LO}^{I} \frac{\exp(-q^2L^2/4a^2)}{[(a)\ \omega(q))^2 + (\Gamma/2)^2]} d^3q, \quad (2)$$

where the phonon dispersion function $\omega(q)$ for an optical branch of crystalline GaAs is given $\omega(q)^2 = A + B\cos(\pi q)$, where A = 269.5 cm"[1] and B = 22.5 cm"[1]. a(5.65A) is the lattice constant. The values of ω and Γ are taken as 291 and 3.5 cm"[1], respectively, corresponding to the first-order Raman line in the crystalline GaAs. The L is the quantum confinement dimension. We have chosen a Gaussian weighing function $\{\exp(-q^2L^2/4a^2)\}$ appropriate quantum confinement [26,27] in Eq. (2). The $N(L)$ is a function included to account for the size distribution of the nanocrystallites, which cause an additional broadening of the Raman mode. This factor is considerably significant for nanocrystals produced by laser-induced etching and is taken to be a Gaussian of the form, $N(L) \approx [\exp - (L - L0)/\sigma^2]$. It is thus determined by the two parameters L0 and σ, where L0 is the most probable or average size of the nanocrystals and σ defines the width of distribution. It turns out from Eq. (2) that the peak positions of the Raman line are mainly determined by *L0,* where *N(L)* is maximum. In etched GaAs samples for excitation energy 2.54 eV, choosing L0 = 50 Å, gives a peak position close to the observed value 288 cm"[1]. For our calculations, we choose a minimum value of $L1$ = 35 Å and varied the values of L_2 and σ to fit experimental data. Similarly, for excitation energy 2.71 eV, L0 is chosen as 40 Å and the minimum value of $L1$ = 20 Å is considered. The value of L_2 and σ are varied to fit the experimental data and it gives a peak position at 287 cm"[1], which is also very close to the observed data. Best fit values of L_2 and σ for both photon energies of 2.54 and 2.71 eV are given in Table 2 and the spectra calculated are shown by the solid line curves in Fig. 5(b). For 2.71 eV of photon energy, the L_2 = 80, σ = 40 Å, and the asymmetry ratio of 3.1 indicates that there is preponderance of small size nanocrystallites with L < 80 Å. The full width at half maximum is 13.5 cm"[1], which is fairly large. For 2.54 eV of photon energy, the penetration depth increases due to decrease in the

Table 2
Theoretically best fit values for *L1* (the minimum confinement dimension), *L2* (the maximum confinement dimension), *L0* (mean value), σ (Gaussian distribution standard deviation) used in Eq. (2) and experimentally measured FWHM and Raman peak position for the first-order Raman mode

Excitation energy (eV)	Theoretically calculated				Experimentally measured	
	L0 (Å)	*U* (Å)	*L2* (Å)	a (Å)	Raman peak position (cm^{-1})	FWHM (cm^{-1})
2.54	50	35	100	50	288	8.5
2.71	40	20	80	50	287	13.5

absorption coefficient of the material. In this case a good fit is obtained for L2 = 100 Å, while σ remains unchanged at 50 Å with the FWHM being 8.5 cm^{-1}. Large nanocrystals are observed at this photon energy value:

It is also observed that the results of Raman spectra provide the size distribution in the range between 40 and 50 Å where as the PL results indicate the size distribution in the range between 35 and 54 Å. There is a slight discrepancy between these investigating methods of size distribution. Difference in the minimum and maximum dimension of nanocrystallites values is roughly 5 Å. Therefore, it is concluded that the laser-induced etching can be used to produce GaAs nanocrystals and it is simplest way to produce a number of nanostructures.

5. Conclusions

Laser-induced etching process can be used to etch GaAs wafer in HF solution without any external biasing and it is evident from the changes in surface morphology shown in SFM micrograph. The morphology can be qualitatively investigated by analyzing the PL and Raman spectra in terms of Gaussian distribution of nanocrystallites sizes with quantum confinement models. Broad PL spectrums with FWHM 300 meV consisting of two bands are explained by existing quantum confinement model assuming two Gaussian distributions. The calculation indicates that the two Gaussian distributions represent different set of nanocrystallites with different origin. The origin of different luminescent bands is discussed. It is found that there is a good correlation between the appearance of red PL band at 1.8 eV and the presence of GaAs nanocrystallites with dimensions ranging from 35 to 54 Å Similarly, Raman spectra of the etched GaAs samples are also analyzed with phonon confinement model. The mean nanocrystallites size determined from line-shape fitting varies between 40 and 50 Å.

For the fabrication of the GaAs nanostructure based devices, it is important to control the size of nanocrystal as well as to develop a reliable means of monitoring the size distributions of the nanocrystallites in these luminescent materials. The studies reported here provide important information's regarding both the growth process and vibrational properties of nanostructures of GaAs materials. Finally, it is demonstrated that laser-induced etching can be used to the synthesis of GaAs nanocrystals. Raman and PL spectroscopics are the most powerful method for the characterization of nanostructures.

Acknowledgements

We are grateful to Professor K.P Jain and Professor S.C. Abbi for many useful discussions. Financial support from the Department of Science and Technology, Government of India, under the project "Raman spectroscopy and Photoluminescence of laser etched Semiconductors" is gratefully acknowledged. Technical support from Mr N.C. Nautiyal is also acknowledged.

References

[1] L.T. Canham, Appl. Phys. Lett. 57 (1990) 1046.
[2] Y. Kanemitsu, H. Tanaka, T. Kushida, K.S. Min, H.A. Atwater, J. Appl. Phys. 86 (1999) 1762.
[3] L. Ngan, K.C. Lee, K.W. Cheah, J. Appl. Phys. 83 (1998) 1637.
[4] H.S. Mavi, B.G. Rasheed, A.K. Shukla, S.C. Abbi, K.P. Jain, J. Phys. D 34 (2001) 292.
[5] N. Noguchi, I. Suemune, Appl. Phys. Lett. 62 (1993) 1429.
[6] N. Yamamoto, A. Sumiya, H. Takai, Mater. Sci. Eng. B. 69-70 (2000) 205.
[7] B.Y Han, C.Y Cha, J.H. Weaver, J. Vac. Sci. Technol. A 16 (1998) 490.
[8] C.Y. Cha, B.Y. Han, J.H. Weaver, Surf. Sci. 381 (1997) L636.
[9] M. Takai, S. Hara, C. Lee, A. Kinomurra, T. Lohner, Nucl. Instrum. Methods B 85 (1994) 752.
[10] V. Svorcik, V. Rybka, Chem. Phys. Lett. 164 (1989) 549.
[11] D.V. Podlesnik, H.H. Gilgen, R.M. Osgood Jr., Appl. Phys. Lett. 48 (1986) 496.
[12] L. Pavesi, M. Guzzi, J. Appl. Phys 75 (1994) 4779.
[13] R. Ashoken, K.P. Jain, H.S. Mavi, M. Balkanski, J. Appl. Phys. 60 (1986) 1985.
[14] E. Grilli, M. Guzzi, R. Zamboni, L. Pavesi, Phys. Rev. B 45 (1992) 1638.
[15] J. Perriere, E. Millon, M. Chamarro, M. Morcrette, C. Andreazza, Appl. Phys. Lett. 78 (2001) 2949.
[16] Y. Kanemitsu, H. Tanaka, T. Kushida, K.S. Min, H.A. Atwater, Physica E 7 (2000) 322.
[17] Y Kanemitsu, H. Tanaka, S. Mimura, T. Kushida, J. Lumin. 83 (1999) 301.
[18] Y Kanemitsu, H. Tanaka, Y Fukunishi, T. Kushida, K.S. Min, H.A. Atwater, Phys. Rev. B 62 (2000) 5100.
[19] R. Ding, H. Wang, Mater. Chem. Phys. 77 (2002) 841.
[20] C.M. Finnie, X. Li, P.W. Bohn, J. Appl. Phys. 86 (1999) 4997.

[21] J. Sabataityte, I. Simkiene, R.A. Bendorius, K. Grigoras, V. Jasutis, V. Pacebutas, H. Tvardauskas, K. Navdzius, Mater. Sci. Eng. C 19 (2002) 159.
[22] T. Suemoto, K. Tanaka, A. Nakajima, T. Itukura, Phys. Rev. Lett. 70 (1993) 3659.
[23] H. Yorikawa, S. Muramatsu, Appl. Phys. Lett. 71 (1997) 644.
[24] D. Zhu, L. Zheng, X. Li, Y. Zang, J. Appl. Phys. 86 (1999) 692.
[25] D.E. Aspnes, A.A. Studna, Phy. Rev. B 27 (1983) 985.
[26] H. Richter, Z.P. Wang, L. Ley, Solid State Commun. 39 (1981) 625.
[27] I.H. Campbell, P.M. Fauchet, Solid State Commun. 58 (1986) 739.